

# DESIGN CONSIDERATIONS FOR A PEBB-BASED MARX-TOPOLOGY ILC KLYSTRON MODULATOR\*

K. Macken<sup>‡</sup>, T. Beukers, C. Burkhart, M.A. Kemp, M.N. Nguyen, and T. Tang

SLAC National Accelerator Laboratory  
2575 Sand Hill Road  
Menlo Park, CA 94025, U.S.A.

## Abstract

The concept of Power Electronic Building Blocks (PEBBs) has its origin in the U.S. Navy during the last decade of the past century. As compared to a more conventional or classical design approach, a PEBB-oriented design approach combines various potential advantages such as increased modularity, high availability and simplified serviceability. This relatively new design paradigm for power conversion has progressively matured since then and its underlying philosophy has been clearly and successfully demonstrated in a number of real-world applications. Therefore, this approach has been adopted here to design a Marx-topology modulator for an International Linear Collider (ILC) environment where easy serviceability and high availability are crucial. This paper describes various aspects relating to the design of a 32-cell Marx-topology ILC klystron modulator. The concept of nested droop correction is introduced and illustrated. Several design considerations including cosmic ray withstand, power cycling capability, fault tolerance, etc., are discussed. Details of the design of a Marx cell PEBB are included.

## I. INTRODUCTION

Well over a decade ago, the U.S. Navy started exploring a new design paradigm for power electronic converters based on the use of standardised building blocks (so-called PEBBs) [1].

This approach has had a far-reaching impact on the design and manufacturing of today's power electronic converters, principally in the higher power and voltage ranges (see e.g. [2,3]).

The PEBB concept is a platform-based approach and presents a valuable alternative to conventional power electronic converter design in terms of reduced complexity. The use of standardised building blocks with well defined functionality and interfaces has been identified as a promising technology to simplify converter design and assembly, thereby reducing overall engineering effort. Modular and hierarchical design principles are key in a PEBB-oriented design.

Figure 1 illustrates a PEBB. Referring to [2,3], the

functionality of a PEBB as a building block is defined as power conversion including:

- power supply for gate drivers & sensors,
- stack or module assembly including gate drivers,
- voltage, current and temperature sensors (including A/D conversion of sensor signals),
- switching control including pulse generation for gate driver,
- communication with control, and
- primary protection.

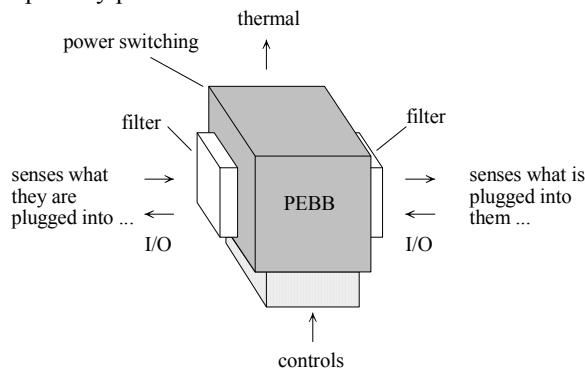


**Figure 1.** Illustration of a PEBB. Power, thermal and control interfaces are standardised.

PEBBs are configured together to form a system. The integration of these PEBBs has to produce the desired system behaviour and performance.

A PEBB-based design approach opens opportunities for increased levels of modularity and compactness. This design paradigm tends to be ideally suited for applications where easy serviceability and high availability are key, such as the ILC.

The aim of this paper is to discuss design considerations in the context of a Marx-topology modulator intended to power an ILC klystron; 120 kV, 140 A, 1.6 ms pulses at a repetition rate of 5 Hz. The concept of nested droop correction is introduced and illustrated in section II. Section III covers various reliability oriented design issues. Details of the design of a Marx cell PEBB are discussed in section IV. Finally, conclusions are given in section V.

\* Work supported by the U.S. Department of Energy under contract DE-AC02-76SF00515

<sup>‡</sup> email: [kmacken@slac.stanford.edu](mailto:kmacken@slac.stanford.edu)

## II. BASIC CONCEPTS

### A. Proposed “Nested” Droop Correction

It is required that the voltage supplied to the cathode of an ILC klystron is kept within  $\pm 0.5\%$  over the pulse duration. Conventional methods to compensate for the output voltage droop that results from the discharge of the storage capacitors in a Marx modulator are based on the use of delayed cells oftentimes in conjunction with additional Vernier cells. However, none of the methods described in the literature are modular in nature as such.

In order to fully exploit the potential benefits of redundancy and fault tolerance inherent to a PEBB-oriented design, a modular approach to droop correction is desirable.

This can be achieved with the topology shown in Figure 2. It is composed of a main cell and a correction cell. Both cells consist of an energy storage capacitor, a charge switch (right switch) and a discharge switch (left switch) and are topologically equivalent to the original cell structure described in [4]. The correction cell is nested at the bottom of the main cell through an output filter (indicated by the shaded area in Figure 2).

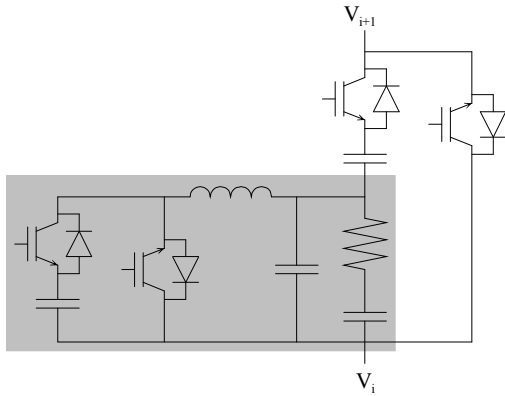


**Figure 2.** Schematic diagram of a basic Marx cell with “nested” droop correction. This concept allows the cell output voltage to be regulated within the specified flatness tolerance over the pulse duration. Some elements (such as charge and isolation diodes) are not shown explicitly.

Pulse energy to the klystron load is predominantly provided by the main cell, as the name implies. Only a small portion of it is delivered by the correction cell.

The correction cell is operated at a significantly lower cell voltage than the main cell. The correction cell can thus be seen as a Vernier-like cell, but unlike a Vernier cell, the correction cell is PWM regulated. It outputs a corrective voltage to compensate for the capacitor voltage droop on the main cell during its discharge, maintaining the combined output voltage of both cells within the specified flatness tolerance.

In this way, a fully modular approach to droop correction is achieved.

The main cell with integrated correction cell as drawn in Figure 2 defines the PEBB also referred to as the Marx cell

PEBB in the remainder of this paper.

A schematic diagram of a Marx modulator built around  $N$  such stacked cells is shown in Figure 3.

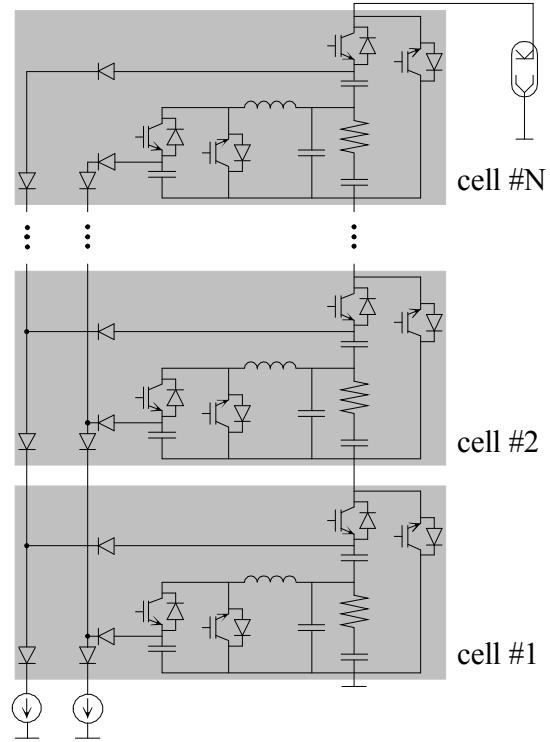


**Figure 3.** Schematic diagram of a  $N$ -cell Marx modulator. A Marx cell can be bypassed through the freewheeling diode of the charge switch in the main cell in case the Marx cell is not fired.

### B. Simulation Results

Figure 3 shows simulated waveforms illustrating the proposed droop correction concept. Simulations were developed using PSIM.

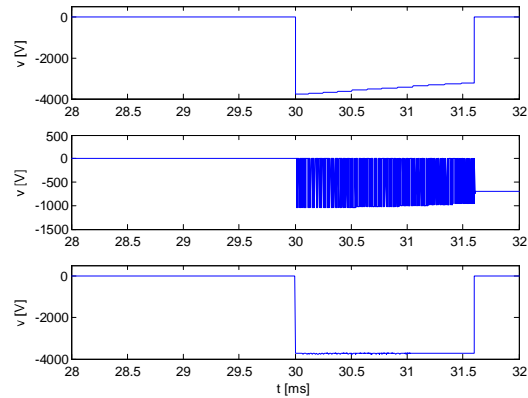


**Figure 3.** Simulated waveforms of voltage across main capacitor (top), on/off modulated corrective voltage (middle) and cell output voltage (bottom) for the circuit of Figure 2.

The initial voltage on the main capacitor (refers to the capacitor in a main cell, likewise correction capacitor refers to the capacitor in a correction cell) is 3750V and the initial voltage on the correction capacitor is 1050 V. The cell output voltage is regulated at 3750 V within the specified flatness tolerance by the correction cell.

The values used in the simulation are chosen based on the considerations developed in section IV.

### III. DESIGN FOR RELIABILITY

#### A. Cosmic Ray Withstand Capability

It is well known that the life of high voltage semiconductor devices can be drastically shortened when exposed to high blocking voltages due to a failure mechanism initiated by cosmic rays [5,6]. This limits the maximum allowable DC blocking voltage for high voltage semiconductor devices to far less than the rated collector-emitter voltage of the device.

The DC blocking voltage at which the occurrence of failures due to cosmic rays is acceptably rare determines its maximum practical operating voltage.

Typically, a failure rate of 100 FIT (1 FIT = 1 failure in  $10^9$  operating hours) is considered to be sufficiently low.

Figure 4 shows the predicted failure rate as a function of DC voltage for a number of 6.5 kV IGBTs.

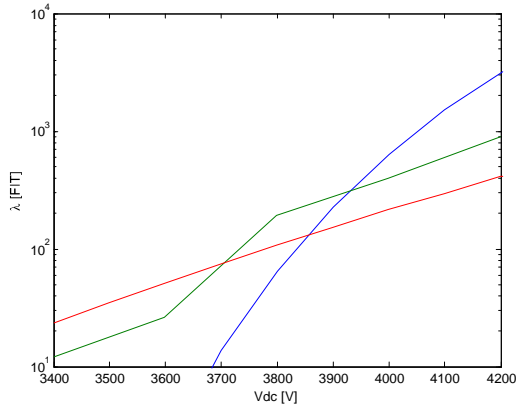


**Figure 4.** Failure rate versus DC voltage at 25°C and sea level.

#### B. Partial Discharge and Insulation Requirements

Partial discharge and insulation requirements are challenging for high voltage semiconductor devices [7].

The IGBT and the diode chips are soldered on a Direct Copper Bonding (DCB) substrate. The DCB substrate is composed of an AlN ceramic, clad on both sides with a patterned Cu layer. The AlN ceramic provides the internal insulation. The insulating substrate is soldered on a base plate, which can be either of Cu or AlSiC. The module is filled with silicone gel to protect the wire bond soldering [8].

A poor insulation between the terminals and base plate of a module significantly reduces its reliability. Partial discharges in the silicone gel should be reduced to acceptable levels in order to avoid electrical degradation of the insulation. Such discharges may occur when using non-qualified semiconductor devices and significantly reduce the device operational lifetime.

Figure 5 specifies the insulation and partial discharge test cycles for 6.5 kV IGBT modules according to IEC 61287 [9].

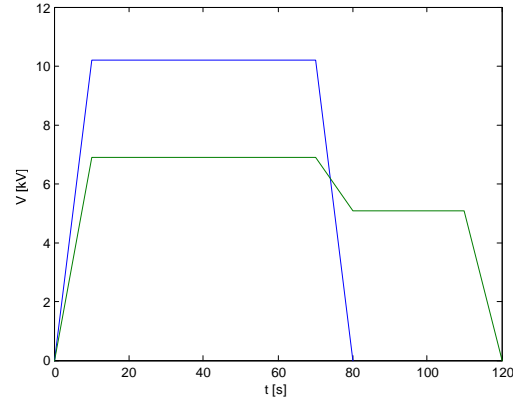


**Figure 5.** Insulation and partial discharge test cycles as required by IEC 61287.

The insulation test cycle (blue graph in Figure 5) demands a voltage of 10.2 kV during 60 s. The partial discharge test cycle (green graph in Figure 5) requests a voltage of 6.9 kV applied for 60 s which is subsequently decreased to 5.1 kV and applied for another 30 s. Partial discharges are measured during the final 5 s of the 30 s time span. The partial discharge level shall be less than 10 pC.

#### C. Power Cycling Capability

Power cycling refers to temperature cycling of the bond wire connections.

Power cycling stresses the bond wires thermo-mechanically causing fatigue. Fatigue of the bond wires leads to bond wire lift off, i.e. loss of contact between bond wires and silicon die. This leads to increased on state voltages [10,11].

A Coffin-Manson relationship can be used to estimate the number of cycles to failure  $N_f$  for a specific temperature cycling amplitude  $\Delta T_j$  as follows

$$N_f = \frac{c}{\Delta T_j^\gamma} \quad (1)$$

where  $c$  and  $\gamma$  are material dependent constants.

Figure 6 shows an example of the estimated number of cycles to failure as a function of the temperature range.

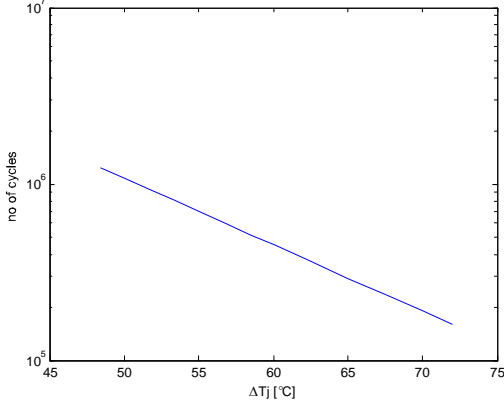


**Figure 6.** Typical curve showing power cycling capability of high voltage IGBT modules from a specific device manufacturer. The number of cycles to failure has a power-law dependence on the temperature cycling amplitude.

Constants  $c$  and  $\gamma$  in (1) can be obtained easily from the curve in Figure 6 as follows

$$c = \frac{N_{f,a}}{\Delta T_{j,a}^{-\gamma}} \quad (2)$$

$$\gamma = \frac{-\ln\left(\frac{N_{f,a}}{N_{f,b}}\right)}{\ln\left(\frac{\Delta T_{j,a}}{\Delta T_{j,b}}\right)} \quad (3)$$

where subscripts  $a$  and  $b$  denote conditions at chosen points  $a$  and  $b$  on the curve, respectively.

A minimum lifetime of  $10^5$  hours is typically targeted for pulsed power applications and is also considered here.

The number of load cycles  $N_{cyc}$  during the expected lifetime is obtained as follows

$$N_{cyc} = 100000 \text{ h} \times 60 \text{ min} \times \frac{60 \text{ s}}{0.2 \text{ s}} = 1.8 \cdot 10^9 \quad (4)$$

For instance, assuming that the junction temperature cycles between  $40^\circ\text{C}$  and  $55^\circ\text{C}$ , which are typical conditions for the discharge switch of the correction cell in the circuit of Figure 2, the number of cycles to failure is estimated at  $8.748 \cdot 10^8$  using (1)-(3) in combination with a power cycling capability curve similar to the one shown in Figure 6.

However, since the device junction is operated at maximally  $55^\circ\text{C}$  instead of  $125^\circ\text{C}$ , a correction for temperature dependence has to be made. Details of how to correct for temperature are not included here for the sake of brevity. The number of cycles to failure rises to  $8.748 \cdot 10^9$ , which is equivalent to  $4.86 \cdot 10^5$  hours and well above the design target.

#### D. Fault Tolerance

In order to tolerate (cell) failures and avoid costly

downtimes, redundancy has to be incorporated into the design of the modulator. As mentioned earlier, a PEBB-oriented design is ideally suited to achieve that objective.

Redundancy can be achieved through a  $k$ -out-of- $n$  system design [12].

The reliability function  $R_{k/n}$  of a  $k$ -out-of- $n$  system can be mathematically expressed as

$$R_{k/n}(t) = \sum_{i=k}^n \frac{n!}{(n-i)!i!} (e^{-\lambda t})^i (1 - e^{-\lambda t})^{n-i} \quad (5)$$

where  $\lambda$  is failure rate.

It should be noted that beyond incorporating redundancy in the design, appropriate fault detection, isolation and reconfiguration mechanisms are equally important to achieve fault-tolerant operation. The interested reader is referred to [13] for a discussion of the principles related to fault tolerance.

## IV. OVERVIEW OF MARX CELL PEBB DESIGN

### A. Choice of Cell Operating Voltage(s)

It is desirable to operate the PEBBs at the highest voltage possible (but without making use of any switch assemblies that consist of series connected semiconductor devices) to limit the number of PEBBs required to construct the Marx modulator.

Driven by the continual evolution in performance and characteristics since its introduction in the early 1990s, the IGBT has become the device of choice for a wide range of medium to high voltage applications.

Today 6.5 kV IGBT modules up to currents of 600 A are commercially available (see e.g. [14]) as illustrated in Figure 7. The lowest current rating is 200 A.

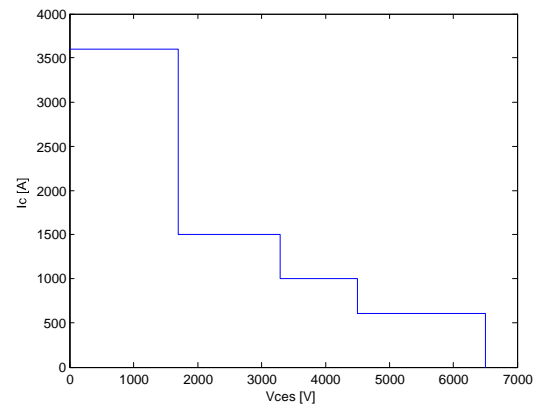


**Figure 7.** Voltage and current ratings range of commercially available high voltage IGBT modules.

From Figure 4 it is clear that a suitable voltage for the main capacitor of a Marx cell PEBB ranges typically between 3400-4000 V, to achieve sufficiently low failure

rates for the 6.5 kV IGBTs.

For instance, a curve fit to the blue graph in Figure 4 yields the following expression to estimate the DC voltage  $V_{dc}$  for a given failure rate  $\lambda$

$$V_{dc} = C_1 - \frac{C_2}{\ln\left(\frac{\lambda}{C_3}\right) - \frac{25 - T_j}{47.6} - \frac{1 - \left(1 - \frac{h}{44300}\right)^{5.26}}{0.143}} \quad (6)$$

where  $T_j$  is junction temperature,  $h$  is altitude, and  $C_1$ ,  $C_2$ , and  $C_3$  are curve fit parameters.

To achieve a negligible failure rate of 100 FIT it follows from (6) that the DC voltage should be limited to 3833 V.

The corresponding repetitive blocking voltage  $V_{dr}$  can be calculated as follows

$$V_{dr} = 1.5V_{dc} \quad (7)$$

and equals 5749.5 V.

Both of the other curves in Figure 4 clearly show failure rates of 100 FIT at similar voltages.

Based on the assumption that the DC voltage should be around 3800 V for reliable long-term performance, a 32-cell design is considered to generate the 120 kV pulse.

For an assumed cell reliability,  $R_{cell}$ , of 99%, it follows from (5) that the reliability of a 32-cell Marx modulator,  $R_{marx}$ , drops to 72.5% if no failures can be tolerated as seen in Figure 8.

Referring to the previous section, tolerance for cell failures can be obtained through a  $k$ -out-of- $n$  design.

Then, the reliability increases to 95.93% (which is still below the reliability of one cell) if one failure can be tolerated and the reliability increases to 99.6% if two failures can be tolerated.

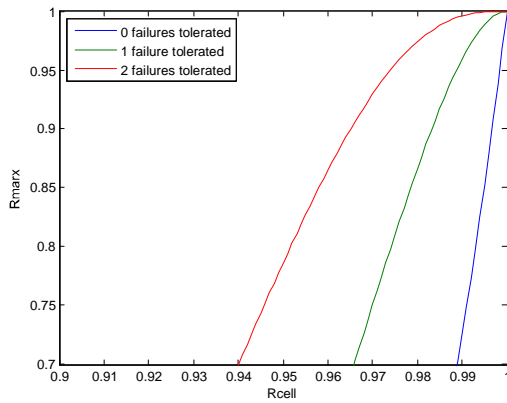


**Figure 8.** Reliability of a 32-cell Marx modulator versus the reliability of one basic Marx cell PEBB.

Tolerating two PEBBs to fail implies that the remaining 30 PEBBs operate at 4000 V. This increased voltage falls within the range as indicated above.

In view of the above considerations, a 32-cell design with  $(N+2)$  redundancy is chosen. The corresponding voltage on the main capacitor of a Marx cell PEBB is 3750 V.

As indicated previously, the correction cell is operated at a significantly lower voltage as compared to the main cell. It is found that a charge voltage of 1050 V is sufficient for the correction capacitor to provide droop correction on the corresponding main capacitor. In consequence, 1.7 kV IGBTs can be selected. As mentioned previously, cosmic ray withstand places a practical upper limit on DC blocking voltage. A maximum voltage of 1070 V is typical for 1.7 kV IGBTs.

### B. (Required) Stored Energy

An ILC klystron requires 26.9 kJ delivered every pulse.

The main capacitors are dimensioned to deliver most of that energy. The correction capacitors, however, are sized to deliver only the energy needed to correct for the voltage droop on the main capacitor in their respective Marx cell PEBB. In this way the size of the main capacitors can be kept within affordable limits.

A smaller main capacitor requires more correction, but a larger capacitor increases its costs. Typically, a 20-40% droop in voltage yields a cost-effective design.

The required size  $C$  of the energy storage capacitors can be calculated as follows

$$C \geq \frac{\tau_p I}{\delta V} \quad (8)$$

where  $\tau_p$  is pulse duration,  $V$  is capacitor voltage,  $I$  is current supplied to the klystron load, and  $\delta$  is voltage droop.

The values obtained for main and correction capacitors using (8) are 350  $\mu$ F and 875  $\mu$ F, respectively, assuming 100  $\mu$ s rise and fall and accounting for 5% age loss and  $\pm 5\%$  tolerance.

Consequently, the main capacitor stores 2460.9 J and the correction capacitor stores 482.3 J.

In short, this design allows 28.6% of the total stored energy in the 32-cell Marx modulator, 94.2 kJ, to be delivered in the output pulse, 26.9 kJ, while keeping the droop within a  $\pm 0.5\%$  range.

### C. Mechanical Construction

A possible assembly of a Marx cell PEBB is illustrated in Figure 9.

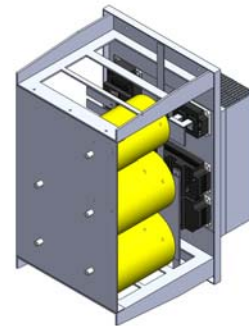


**Figure 9.** View of possible assembly of Marx cell PEBB showing the impact of the energy storage capacitors on the overall size of the cell.

Semiconductor devices and energy storage capacitors are selected based upon the considerations described above. The size of the cell is to a significant extent dictated by the energy storage capacitors. Metallised polypropylene film capacitors are used. An energy density of about 0.25 J/cc was conservatively selected for the capacitors. More effort is currently underway to determine the optimal energy density of these capacitors in an ILC context.

## V. CONCLUSIONS

This paper provided guidance for the design of a PEBB-based Marx-topology ILC klystron modulator. The concept of nested droop correction was introduced and illustrated through simulation. Various design considerations were addressed. Details of the design of a Marx cell PEBB were given. It was shown that a suitable voltage for the main capacitor of a Marx cell PEBB ranges typically between 3400-4000 V. A 32-cell design with (N+2) redundancy was chosen, requiring 3750 V on the main capacitor of each Marx cell PEBB. A charge voltage of 1050 V was found to be sufficient for the correction capacitor to provide droop correction on the corresponding main capacitor. It was calculated that the main capacitor stores 2460.9 J and the correction capacitor stores 482.3 J. Clearly, this design allows 28.6% of the total stored energy in the 32-cell Marx modulator, 94.2 kJ, to be delivered in the output pulse, 26.9 kJ, while keeping the droop within a  $\pm 0.5\%$  range.

## REFERENCES

- [1] T. Ericson, "Power Electronic Building Blocks - A systematic approach to power electronics," in *Proc. Power Engineering Society Summer Meeting*, Seattle, WA, July 16-20, 2000, pp. 1216-1218.
- [2] T. Ericson, Y. Khersonsky, P. Schugart, and P. Steimer, "PEBB - Power Electronics Building Blocks, from concept to reality," in *Proc. Int. Conference on Power Electronics, Machines and Drives*, Dublin, Ireland, Apr. 4-6, 2006, pp. 12-16.
- [3] P.K. Steimer, B. Ødegård, O. Apeldoorn, S. Bernet, and T. Brückner, "Very high power IGCT PEBB technology," in *Proc. IEEE Power Electronics Specialists Conference*, Recife, Brazil, June 12-16, 2005, pp. 1-7.
- [4] R.L. Cassel, "High voltage pulsed power supply using solid state switches," U.S. Patent 7 301 250, Nov. 27, 2007.
- [5] N.Y.A. Shamma, "Present problems of power module packaging technology," *Microelectronics Reliability*, vol. 43, pp. 519-527, April 2003.
- [6] H.R. Zeller, "Cosmic ray induced failures in high power semiconductor devices," *Microelectronics and Reliability*, vol. 37, pp. 1711-1718, Oct.-Nov. 1997.
- [7] G. Mitic, T. Licht, and G. Lefranc, "IGBT module technology with high partial discharge resistance," in *Proc. IEEE Industry Applications Conference*, Chicago, IL, Sept. 30-Oct. 4, 2001, pp. 1899-1904.
- [8] W.W. Sheng and R.P. Colino, *Power electronic modules: design and manufacture*. Boca Raton, FL: CRC Press, 2004.
- [9] "Railway applications - Power convertors installed on board rolling stock - Part 1: Characteristics and test methods," IEC 61287-1, 2005.
- [10] M. Held, P. Jacob, G. Nicoletti, P. Scacco, and M.-H. Poech, "Fast power cycling test of IGBT modules in traction application," in *Proc. Int. Conference on Power Electronics and Drive Systems*, Singapore, May 26-29, 1997, pp. 425-430.
- [11] M. Ciappa, "Selected failure mechanisms of modern power modules," *Microelectronics Reliability*, vol. 42, pp. 653-667, Apr.-May 2002.
- [12] K.J.P. Macken, I.T. Wallace, and M.H.J. Bollen, "Reliability assessment of motor drives," in *Proc. IEEE Power Electronics Specialists Conference*, Jeju, Korea, June 18-22, 2006, 7 pp.
- [13] R.V. White and F.M. Miles, "Principles of fault tolerance," in *Proc. IEEE Applied Power Electronics Conference and Exposition*, San Jose, CA, Mar. 3-7, 1996, pp. 18-25.
- [14] A. Kopta, M. Rahimo, U. Schlapbach, D. Schneider, E. Carroll, and S. Linder, "A 6.5 kV IGBT module with very high safe operating area," in *Proc. IEEE Industry Applications Conference*, Hong Kong, Oct. 2-6, 2005, pp. 794-798.